ICE SHEETS

A dynamic saline groundwater system mapped beneath an Antarctic ice stream

Chloe D. Gustafson[1,2]*, Kerry Key[1], Matthew R. Siegfried[3], J. Paul Winberry[4], Helen A. Fricker[2], Ryan A. Venturelli[5], Alexander B. Michaud[6]

Antarctica's fast-flowing ice streams drain the ice sheet, with their velocity modulated by subglacial water systems. Current knowledge of these water systems is limited to the shallow portions near the ice-bed interface, but hypothesized deeper groundwater could also influence ice streaming. Here, we use magnetotelluric and passive seismic data from Whillans Ice Stream, West Antarctica, to provide the first observations of deep sub–ice stream groundwater. Our data reveal a volume of groundwater within a >1-kilometer-thick sedimentary basin that is more than an order of magnitude larger than the known subglacial system. A vertical salinity gradient indicates exchange between paleo seawater at depth and contemporary basal meltwater above. Our results provide new constraints for subglacial water systems that affect ice streaming and subglacial biogeochemical processes.

The ice flux from the Antarctic Ice Sheet's interior to its margins is largely governed by the behavior of fast-flowing ice streams [e.g., (*1*)], where the availability of subglacial water plays a fundamental role in regulating ice flow (*2*). Given the inaccessibility of the Antarctic substrate, physical constraints on the sub–ice stream water systems are based on a few geophysical (i.e., active seismic, radar sounding) surveys [e.g., (*3*, *4*)] and subglacial drilling efforts [e.g., (*5*)]. These observations revealed a "shallow" sub–ice stream hydrologic system, which we define here as water at the ice-bed interface (in the form of films, channels, and lakes) and water within a relatively thin (≲10 m) deformable layer of unsorted sediments, generally considered glacial till (*5*). Below these shallow hydrologic systems, Antarctic ice streams are expected to be underlain by sedimentary basins hundreds to thousands of meters thick that have the capacity to host substantial groundwater (*6*), constituting "deep" subglacial hydrologic systems, which we define here as groundwater below the glacial till. These deep groundwater systems have the potential to provide water to or remove water from the ice base and, therefore, may play a role in modulating ice flow (*6*). However, current Antarctic subglacial water models only consider the shallow hydrologic systems, partly because the geophysical tools typically used to map deep sub–ice stream sediments (i.e., active and passive seismics, gravity, and magnetics) (*7*–*9*) do not provide constraints on deep groundwater properties or connectivity between the shallow and deep hydrologic systems. Here, we use magnetotelluric (MT) (*10*) and passive seismic data (*11*, *12*) to provide the first in situ measurements of a deep groundwater system within a >1-km-thick sedimentary basin beneath the West Antarctic Ice Sheet. We infer that this basin contains more than an order of magnitude more water than the shallow hydrologic systems typically considered in subglacial water

[1]Lamont-Doherty Earth Observatory, Columbia University, Palisades, NY, USA. [2]Institute of Geophysics and Planetary Physics, Scripps Institution of Oceanography, University of California, San Diego, La Jolla, CA, USA. [3]Hydrologic Science and Engineering Program, Department of Geophysics, Colorado School of Mines, Golden, CO, USA. [4]Department of Geological Sciences, Central Washington University, Ellensburg, WA, USA. [5]Department of Geology and Geological Engineering, Colorado School of Mines, Golden, CO, USA. [6]Bigelow Laboratory for Ocean Sciences, East Boothbay, ME, USA.
*Corresponding author. Email: cgustafson@ucsd.edu

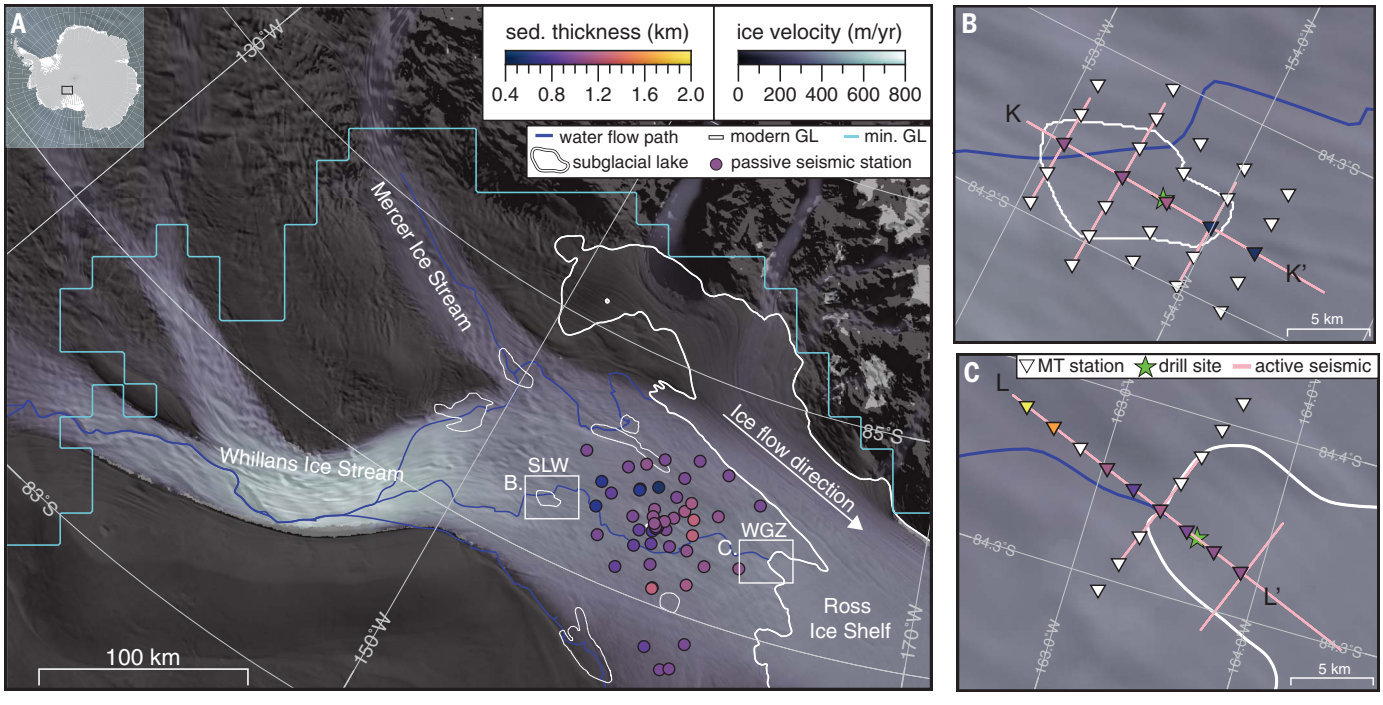

Fig. 1. Regional map of passive seismic and MT surveys on Whillans Ice Stream, West Antarctica. (**A**) WIS ice velocity (*44*) plotted over a satellite image mosaic (*45*) with active subglacial lakes (*20*) and predicted basal water flow paths (*42*) that deliver water across the modern grounding line (GL) (*46*). The estimated most-landward grounding line position after the Last Glacial Maximum (*34*) is shown in cyan (minimum GL, labeled as "min. GL"). Colored circles indicate passive seismic receiver locations and corresponding sediment thickness estimates. (**B** and **C**) MT stations at (B) SLW and (C) WGZ are aligned with previous active-source seismic profiles (*21*, *22*) and sites of direct subglacial drilling access (*23*, *24*). Colored triangles indicate sediment thickness estimates (*24*). 2D inversion results of MT stations K to K' and L to L' are shown in Fig. 2.

models (*13*). The groundwater salinity increases with depth, indicating that the deep and shallow subglacial water systems are hydrologically connected and that Antarctic groundwater may influence ice stream behavior and subglacial biogeochemical processes.

Previous studies have recognized the potential presence of groundwater beneath Antarctic ice streams [e.g., (*6*)]; however, its detection has been challenging. Electromagnetic (EM) methods, which are frequently used for terrestrial groundwater studies (*14*), are also a feasible technique for detecting deep subglacial groundwater (*15*). Variations in resistivity can be exploited to delineate high-resistivity glacier ice (~4×10^4 to 1×10^8 ohm·m) from low-resistivity sediments (~1 to 100 ohm·m) and moderately resistive bedrock (~100 to 1000 ohm·m) (*15*). Furthermore, resistivity variations within groundwater-bearing sediments can provide constraints on water properties because saltier porewater yields a bulk resistivity that is an order of magnitude lower than that of freshwater (*15*). Recent surveys in the McMurdo Dry Valleys have demonstrated the effectiveness of high-frequency airborne EM soundings for mapping groundwater within the top few hundred meters of subglacial environments [e.g., (*16*)] but under only <350 m of ice. Sensing deeper groundwater within sedimentary basins below thicker ice requires ground-based EM methods, such as MT (*15*), a passive EM method that uses natural low-frequency EM fields to image subsurface resistivity at depths spanning from the shallow crust to the upper mantle. MT methods have been widely applied in continental and oceanic settings for constraining subsurface fluid and lithologic distributions (*17*) yet, in Antarctica, have only been used to examine the deep crust and lithosphere (*18*).

We collected MT data (fig. S1) on the downstream outlet of Whillans Ice Stream (WIS), located along Siple Coast (which we use here to collectively describe the Gould, Siple, and Shirase coasts) of West Antarctica (Fig. 1A), to investigate deep groundwater within a sedimentary basin under ~800 m of ice. Numerical simulations have estimated that groundwater considerably contributes to Siple Coast ice streaming, but this modeling only included shallow water volumes and fluxes within the till because there were no observations of deep groundwater to constrain their modeling (*19*). Our MT surveys focused on two hydrologically connected regions that are part of a dynamic subglacial water system (*20*): Whillans Subglacial Lake (SLW) (Fig. 1B) and its hypothesized downstream outlet to the ocean, Whillans Grounding Zone (WGZ) (Fig. 1C). We supplemented our focused MT surveys with a passive seismic survey that was sparser but sampled a wider region, extending across WIS (colored circles in Fig. 1A). At both MT survey locations, the shallow hydrology has been constrained by geophysical surveying (*4*, *21*, *22*) and direct subglacial sampling (*23*, *24*). Although these studies did not image or sample the deeper groundwater, porewater samples from a shallow (0.38 m) sediment core below SLW showed an increasing contribution of seawater-sourced Cl^-, indicating a deeper reservoir of seawater (*25*). The active-source seismic studies (pink lines in Fig. 1, B and C) also revealed that each location is underlain by a substantial thickness

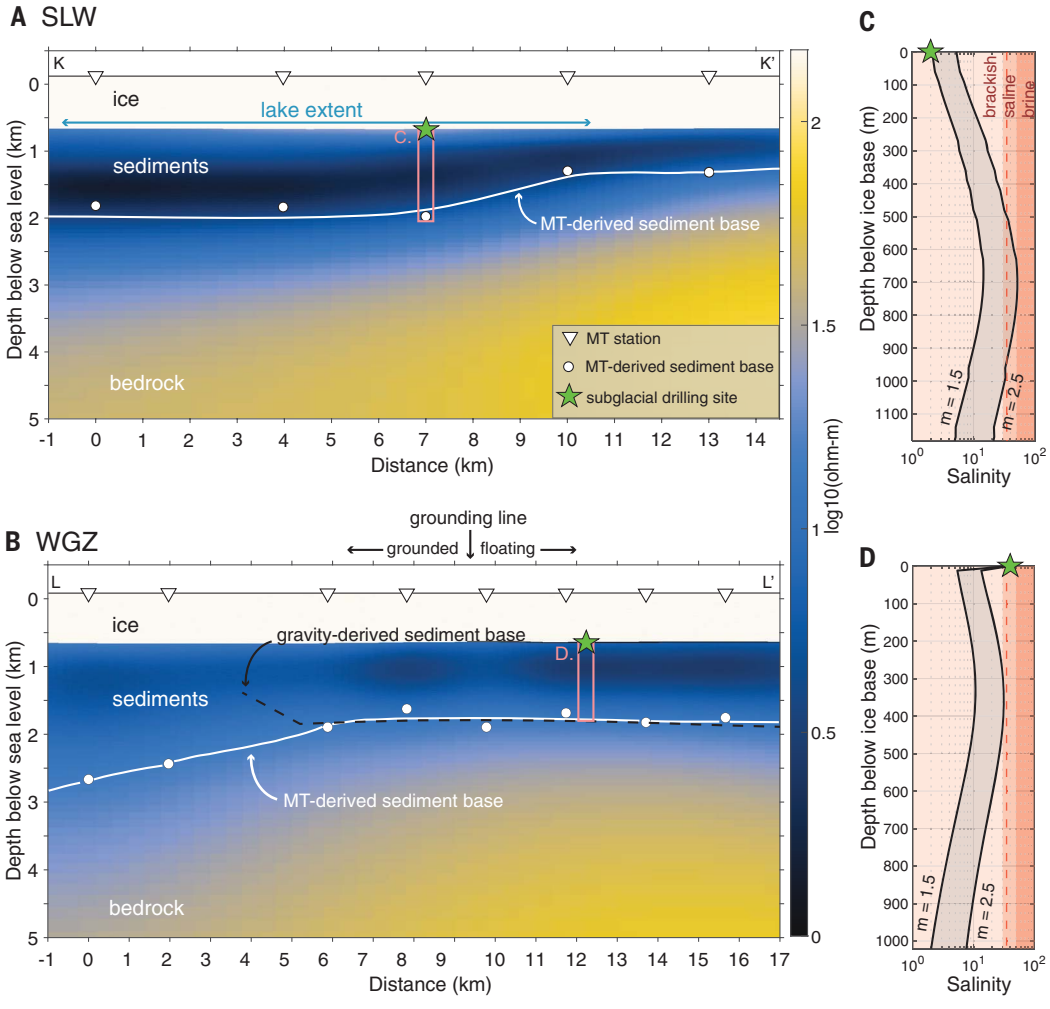

Fig. 2. Resistivity models and inferred groundwater salinity. (**A** and **B**) Electrical resistivity models of (A) SLW and (B) WGZ obtained by 2D regularized inversion (*27*). White circles show the estimated sediment thickness obtained from a 1D Bayesian inversion of each station's data [fig. S4 and (*27*)]. The WGZ model additionally includes a black dashed line noting the base of the sediment layer as interpreted by ground-based gravity surveying (*28*). The deviation between the MT- and gravity-derived sediment base around the 4-km position is likely an edge effect in the gravity inversion. (**C** and **D**) Vertical water salinity profile estimates (gray-shaded region) estimated by applying Archie's law (*27*) to vertical profiles extracted from the 2D resistivity models. Red shading denotes the salinity characterizations using the unitless practical salinity scale [brackish (0.1 to 30), saline (30 to 50), and brine (>50)], whereas the red dashed line denotes seawater salinity (35). The green stars in (A) and (B) note the location of subglacial sediment sampling. In (C), the green star marks the maximum porewater salinity from subglacial sampling of the top 0.38 m of sediments at the same location (*25*), and in (D), the green star indicates the seawater salinity observed in the ocean cavity (*24*).

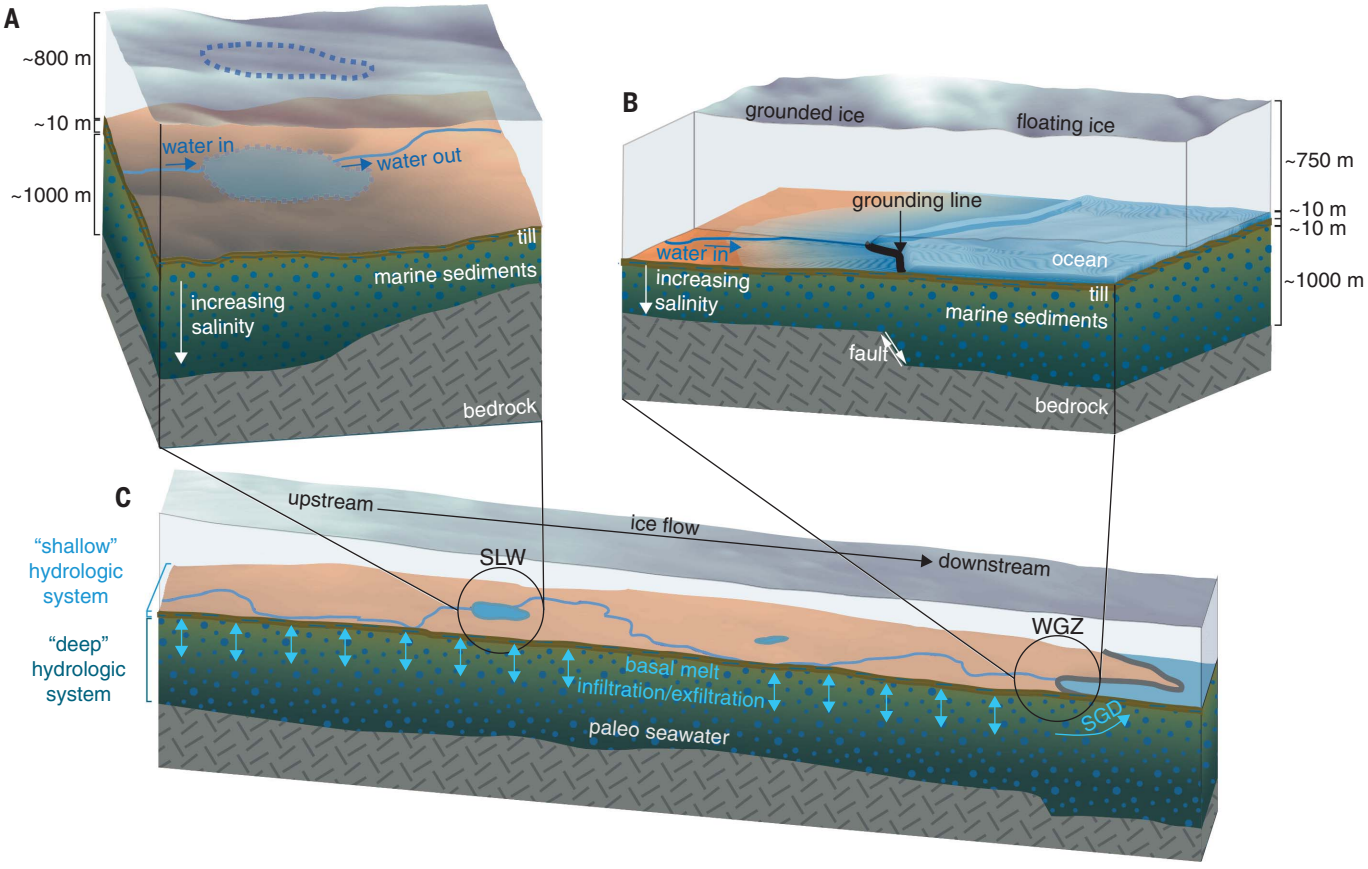

Fig. 3. Conceptual models of WIS groundwater and water routing. (**A** to **C**) Thick sediments that contain groundwater that increases in salinity with depth at both (A) SLW and (B) WGZ are persistent throughout (C) WIS. We attribute the vertical salinity gradient to paleo seawater mixing with contemporary basal meltwater. Low-salinity groundwater in sub–ocean cavity sediments (Fig. 2D) indicates that groundwater flows laterally across the grounding line and enters the ocean as SGD.

of stratified sediments (>100 m) (*22*, *26*) but were not able to conclusively map depth to bedrock (i.e., total sediment thickness) or constrain the deep hydrology.

We determined sediment thickness beneath WIS using passive seismic and MT observations. Our regional passive seismic sediment thickness estimates obtained by receiver function analysis (*27*) (figs. S2 and S3) range from 0.6 to 1.3 km (± 0.2 km) (Fig. 1A), which are consistent with MT-derived sediment thickness estimates that we calculated using one-dimensional (1D) Bayesian inversion methods (*27*) (fig. S4) at SLW (0.5 to 1.2 km ± 0.1 km; Fig. 1B) and at WGZ (0.9 to 1.9 km ± 0.1 km; Fig. 1C). These estimates are in overall agreement with those derived from airborne surveying [e.g., (*7*)] and ground-based gravity surveying (*28*). The Bayesian sediment thickness estimates are also compatible with the structure of the 2D resistivity models that we obtained using regularized inversion for linear profiles of MT stations (*27*), which revealed a low-resistivity layer consistent with water-saturated sediments overlying a more resistive layer consistent with bedrock (Fig. 2, A and B, and figs. S5 and S6).

Information about groundwater contained within the sediments comes from examining resistivity within the sediment layer in our 2D models (blue shading above the white line in Fig. 2, A and B). We used the empirical Archie's law to convert resistivity to groundwater salinity for vertical profiles in our model that are colocated with past subglacial drilling sites at SLW (Fig. 2C) and WGZ (Fig. 2D) (*24*). We assumed a range of Archie's exponents that are appropriate for sedimentary rocks (m = 1.5 to 2.5), a sediment compaction model consistent for porosity observations from the Ross Sea (*29*), and a 50°C/km temperature gradient consistent with heat-flux observations from WIS (*30*). Salinity at the top of the sediment column is brackish (defined here as 0.1 to 30 on the unitless practical salinity scale) for both SLW (2 to 5) and WGZ (5 to 13). At SLW, this range corresponds well with direct porewater salinity measurements [green star in Fig. 2C, and (*25*)]. At WGZ, we constrain our model to include a seawater layer (*24*) that matches observed seawater conductivity [green star in Fig. 2D and (*24*)]. Groundwater salinity increases with depth, to 700 m at SLW and 400 m at WGZ, with the upper bounds at both locations reaching values >30, that is, close to that of seawater (~35). At both locations, the salinity appears to decrease below these depths. However, because MT data cannot resolve a sharp increase in resistivity that would result from low-resistivity salty groundwater in direct contact with high-resistivity bedrock (*14*), we propose that the saltiest groundwater is located at the bottom of the sediment column (Fig. 3, A and B) and the apparent freshening is a result of smoothing in our regularized inversion.

Given the similarity in groundwater salinity and general resistivity structure between SLW and WGZ, we infer that the thick sediments sampled by our passive seismic stations are also saturated with groundwater that increases in salinity with depth (Fig. 3C). If we were to extract this water from the sediments, the water column's equivalent thickness would range from 220 to 820 m, assuming the same porosity model from our Archie's law calculations integrated over the thickness of the sediments estimated from MT and passive seismic data (0.4 to 1.9 km) (*27*). This demonstrates that the volume of deep groundwater is

at least an order of magnitude greater than the water in shallow sub–ice stream hydrologic systems [~2 to 15 m for Siple Coast ice stream subglacial lakes (*31*, *32*) and ~3-m equivalent water depth for the till (*13*)].

The upward freshening of groundwater provides information about the glacial and hydrologic processes that led to the development of the groundwater system, as well as the extent of the system. We propose that the salty porewater within the deepest sediments is of marine origin, which is consistent with geochemistry from the shallow subglacial system at SLW (*25*). The most recent marine incursion at WIS occurred in the mid-Holocene (*33*) following the Last Glacial Maximum deglaciation, when the grounding line retreated inland of its modern position, upstream of SLW (*34*) (cyan line in Figs. 1A and 4). We propose that this resulted in seawater rapidly convecting downward to the base of the preexisting sediments [fig. S7 and (*27*, *35*)] beneath WIS and other Siple Coast ice streams (cyan hatching in Fig. 4) that experienced the same marine incursion (*33*, *34*). Some deep salty water may also be left over from when the sediments were initially deposited under open-ocean conditions when West Antarctica was ice free (*36*); this older water possibly extends upstream to the onset of ice streaming (blue hatching in Fig. 4). The emplacement of lower salinity water that we observe at the top of the sediments was driven by subsequent grounding line readvance and ice sheet regrowth, which forced fresh basal meltwater into the sediments through ice-sediment hydromechanical feedbacks [e.g., (*37*)].

Infiltration of basal meltwater into the top few hundred meters of sediments demonstrates that the deep and shallow sub–ice stream hydrologic systems are physically connected. This connection has been suggested theoretically using hydromechanical models of paleo (*37*) and extant (*38*) ice sheets but has not previously been proven through observations in Antarctica. Although our observed salinity gradients are only indicative of shallow subglacial water infiltrating into the deep hydrologic environment, deep groundwater can also ascend into the shallow system. Because ice thickening promotes water flow into the sediments and ice thinning allows for water to exfiltrate from the sediments and enter the shallow hydrologic environment (*37*), the direction of water flow and the spatiotemporal scales over which flow occurs is dynamically coupled to ice behavior.

The confirmation of the existence of deep groundwater dynamics has transformed our understanding of ice stream behavior and will force modification of subglacial water models. A connection between the deep and shallow subglacial water systems suggests that upward groundwater flow is another potential source of water and heat (*38*), which can enhance basal melting at the ice base. Conversely, downward groundwater flow removes both water and heat from the ice base (*38*), promoting freezing conditions that slow ice flow. The role of groundwater flow may be further complicated by the transport of solutes between the deep and shallow hydrologic systems, which can modify the in situ basal melting point. Given the large groundwater volume that we observe, we propose that future Antarctic sub–ice stream water models incorporate both deep and shallow water systems to determine the importance of groundwater to ice stream dynamics.

The presence and flow of deep groundwater also has implications for subglacial ecosystems and biogeochemical cycles. Our observations of deep paleo seawater suggest that Siple Coast sedimentary basins are marine in origin, and biogeochemical cycles common to deeply buried marine sediments (i.e., methanogenesis) are likely operating and may be responsible for carbon transformation at depth (*39*, *40*). Upward groundwater fluxes may transport the products produced by microbial communities (e.g., dissolved organic or inorganic carbon) to the shallow subglacial systems, where it fuels subglacial ecosystems (*23*, *41*) and can be rapidly transported to the ocean via the shallow hydrologic system (*42*). Deep lateral groundwater flow can also transport this otherwise sequestered carbon directly to the ocean via submarine groundwater discharge (SGD) [e.g., (*43*)]; the low salinity estimated for the sediment groundwater directly beneath the ocean cavity at WGZ (Fig. 2D) suggests that SGD may be occurring [Fig. 3C and (*27*)]. Thus, deep groundwater reservoirs beneath ice streams not only contain saline water indicative of past marine incursions but also likely contain the marine microorganisms and carbon that accumulated when the marine sediments were deposited. Groundwater flow can facilitate the mobilization of sequestered carbon to the ice base and oceans during times of enhanced groundwater exfiltration, thereby increasing Antarctica's contribution of carbon to the ocean. The introduction of water into sub–ice shelf cavities via SGD may also affect ocean circulation and dynamics.

For the past several decades, our understanding of Antarctic sub–ice stream water and its relationship to ice behavior has focused on exchange and transport in the shallow hydrologic environment, whereas the presence and role of deeper groundwater have remained largely unexplored because of the lack of observations. Our MT data provide

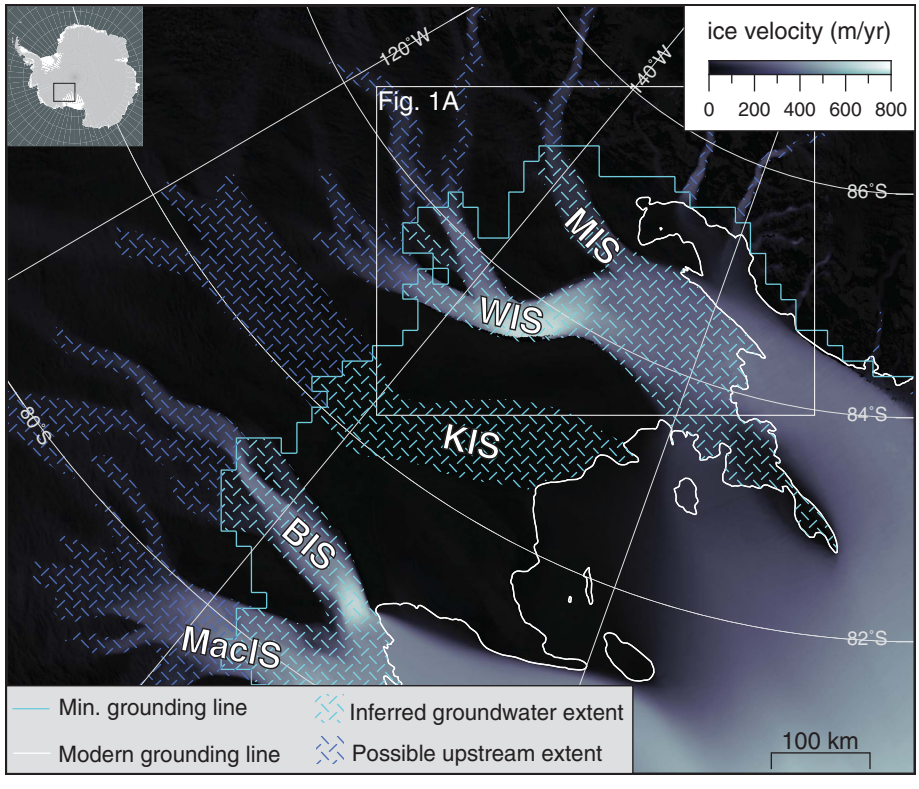

Fig. 4. Potential extent of sub–ice stream deep groundwater systems underlying the Siple Coast. We hypothesize that deep groundwater systems are present within the sedimentary basins underlying Mercer Ice Stream (MIS), WIS, Kamb Ice Stream (KIS), Bindschadler Ice Stream (BIS), and MacAyeal Ice Stream (MacIS). We infer an increase in groundwater salinity with depth (cyan hatching) that possibly extends upstream to the onset of ice streaming (blue hatching).

unequivocal evidence and new constraints for groundwater in a >1-km-thick sedimentary basin. The inferred salinity gradient shows that groundwater represents an active component of the sub–ice stream hydrologic system, redistributing water, heat, solutes, and carbon below WIS. We expect that similar groundwater systems exist within other marine sedimentary basins that underlie Antarctic ice streams, particularly those that have experienced similar episodes of grounding line retreat and readvance, such as in the Siple Coast and Weddell Sea sector (*34*). Understanding the influence of this groundwater on ice sheet behavior will require its integration into the next generation of ice sheet models.

REFERENCES AND NOTES

1. M. R. Bennett, *Earth Sci. Rev.* **61**, 309–339 (2003).
2. M. Bougamont, S. Price, P. Christoffersen, A. J. Payne, *J. Geophys. Res.* **116**, F04018 (2011).
3. D. D. Blankenship, C. R. Bentley, S. T. Rooney, R. B. Alley, *Nature* **322**, 54–57 (1986).
4. K. Christianson, R. W. Jacobel, H. J. Horgan, S. Anandakrishnan, R. B. Alley, *Earth Planet. Sci. Lett.* **331–332**, 237–245 (2012).
5. B. Kamb, in *The West Antarctic Ice Sheet Behavior and Environment*, R. B. Alley, R. A. Bindschadle, Eds. (Antarctic Research Series, vol. 77, American Geophysical Union, 2001), pp. 157–199.
6. M. J. Siegert *et al*., *Spec. Publ. Geol. Soc. London* **461**, 197–213 (2018).
7. R. E. Bell *et al*., *Nature* **394**, 58–62 (1998).
8. S. Anandakrishnan, D. D. Blankenship, R. B. Alley, P. L. Stoffa, *Nature* **394**, 62–65 (1998).
9. M. Studinger *et al*., *Geophys. Res. Lett.* **28**, 3493–3496 (2001).
10. C. Gustafson, H. Fricker, K. Key, M. Siegfried, Wideband magnetotelluric responses from Whillans Ice Stream, West Antarctica. U.S. Antarctic Program (USAP) Data Center (2022); https://doi.org/10.15784/601526.
11. P. Winberry, S. Anandakrishnan, D. Wiens, Geophysical study of ice stream stick-slip dynamics. International Federation of Digital Seismograph Networks (2010); https://doi.org/10.7914/SN/2C_2010.
12. S. Tulaczyk, I. Joughin, S. Schwartz, J. Walter, Elevation change anomalies in West Antarctica and dynamics of subglacial water beneath ice streams and their tributaries. International Federation of Digital Seismograph Networks (2010); https://doi.org/10.7914/SN/1D_2010.
13. T. M. Kyrke-Smith, A. C. Fowler, *Proc. Math. Phys. Eng. Sci.* **470**, 20140340 (2014).
14. R. Kirsch, Ed., *Groundwater Geophysics: A Tool for Hydrogeology* (Springer, 2006).
15. K. Key, M. R. Siegfried, *J. Glaciol.* **63**, 755–771 (2017).
16. N. Foley *et al*., *Hydrology* **6**, 54 (2019).
17. A. D. Chave, A. G. Jones, Eds., *The Magnetotelluric Method Theory and Practice* (Cambridge Univ. Press, 2012).
18. G. J. Hill, *Surv. Geophys.* **41**, 5–45 (2019).
19. P. Christoffersen, M. Bougamont, S. P. Carter, H. A. Fricker, S. Tulaczyk, *Geophys. Res. Lett.* **41**, 2003–2010 (2014).
20. H. A. Fricker, T. Scambos, *J. Glaciol.* **55**, 303–315 (2009).
21. H. J. Horgan *et al*., *Geology* **41**, 1159–1162 (2013).
22. H. J. Horgan *et al*., *Earth Planet. Sci. Lett.* **331–332**, 201–209 (2012).
23. B. C. Christner *et al*., *Nature* **512**, 310–313 (2014).
24. C. B. Begeman *et al*., *J. Geophys. Res. Oceans* **123**, 7438–7452 (2018).
25. A. B. Michaud *et al*., *Geology* **44**, 347–350 (2016).
26. H. J. Horgan, K. Christianson, R. W. Jacobel, S. Anandakrishnan, R. B. Alley, *Geophys. Res. Lett.* **40**, 3934–3939 (2013).
27. Materials and methods are available as supplementary materials.
28. A. Muto, K. Christianson, H. J. Horgan, S. Anandakrishnan, R. B. Alley, *J. Geophys. Res. Solid Earth* **118**, 4535–4546 (2013).
29. R. M. McKay *et al*., "Expedition 374 preliminary report: Ross Sea West Antarctica Ice Sheet history" (International Ocean Discovery Program, 2018).
30. C. B. Begeman, S. M. Tulaczyk, A. T. Fisher, *Geophys. Res. Lett.* **44**, 9823–9832 (2017).
31. S. Tulaczyk *et al*., *Ann. Glaciol.* **55**, 51–58 (2014).
32. J. C. Priscu *et al*., *Ann. Glaciol.* **62**, 340–352 (2021).
33. R. A. Venturelli *et al*., *Geophys. Res. Lett.* **47**, e2020GL088476 (2020).
34. J. Kingslake *et al*., *Nature* **558**, 430–434 (2018).
35. V. E. A. Post, H. Kooi, *Hydrogeol. J.* **11**, 549–559 (2003).
36. R. P. Scherer, *Global Planet. Change* **4**, 395–412 (1991).
37. J. M. Lemieux, E. A. Sudicky, W. R. Peltier, L. Tarasov, *J. Geophys. Res.* **113**, F01011 (2008).
38. B. T. Gooch, D. A. Young, D. D. Blankenship, *Geochem. Geophys. Geosyst.* **17**, 395–409 (2016).
39. A. B. Michaud *et al*., *Nat. Geosci.* **10**, 582–586 (2017).
40. I. P. G. Marshall, S. M. Karst, P. H. Nielsen, B. B. Jørgensen, *Mar. Genomics* **37**, 58–68 (2018).
41. T. J. Vick-Majors *et al*., *Global Biogeochem. Cycles* **34**, 1–17 (2020).
42. S. P. Carter, H. A. Fricker, *Ann. Glaciol.* **53**, 267–280 (2012).
43. T. Uemura, M. Taniguchi, K. Shibuya, *Geophys. Res. Lett.* **38**, L08402 (2011).
44. J. Mouginot, E. Rignot, B. Scheuchl, *Geophys. Res. Lett.* **46**, 9710–9718 (2019).
45. T. A. Scambos, T. M. Haran, M. A. Fahnestock, T. H. Painter, J. Bohlander, *Remote Sens. Environ.* **111**, 242–257 (2007).
46. M. A. Depoorter *et al*., *Nature* **502**, 89–92 (2013).

ACKNOWLEDGMENTS

We thank the Antarctic Support Contract, Kenn Borek Air, New York Air National Guard for logistical support; M. Siefert, our field mountaineer, for ensuring the safety of our field camp and assistance with all MT data collection; Phoenix Geophysics for loaning us MT instrument systems and P. Wannamaker for renting us his electrode and buffer preamplifier systems; D. Blatter for assistance with the Bayesian inversion code; A. Muto and K. Christianson for sharing gravity and radar datasets to assist with our interpretation; S. Adusumilli, B. Kulessa, R. Bell, M. Steckler, and the SALSA Science Team for useful discussions; and S. Naif for initial discussions about the prospect of using MT for shallow subglacial science. **Funding:** This work was funded by National Science Foundation grant OPP-1643917 (K.K., C.D.G., M.R.S., and H.A.F.); National Science Foundation grant OPP-0944794 (J.P.W.); National Science Foundation grant OPP-1914767 (J.P.W.); and the Columbia University Electromagnetic Methods Research Consortium (C.D.G.). **Author contributions:** Conceptualization: C.D.G., K.K., M.R.S., J.P.W., H.A.F.; Methodology: C.D.G., K.K., J.P.W.; Software: C.D.G., K.K., J.P.W.; Validation: C.D.G., K.K., J.P.W.; Formal analysis: C.D.G., K.K., J.P.W.; Investigation: C.D.G., K.K., M.R.S., J.P.W.; Resources: K.K., J.P.W.; Data curation: C.D.G., K.K., J.P.W.; Writing – original draft: C.D.G., K.K., M.R.S., J.P.W., H.A.F.; Writing – review and editing: All authors; Visualization: C.D.G., K.K., M.R.S., J.P.W., H.A.F.; Supervision: K.K., M.R.S., J.P.W., H.A.F.; Project administration: C.D.G., K.K., M.R.S., J.P.W.; Funding acquisition: K.K., M.R.S., J.P.W., H.A.F. **Competing interests:** The authors declare that they have no competing interests. **Data and materials availability:** All MT data that were inverted and analyzed in this study are available at the US Antarctic Program Data Center (*10*). All seismic data analyzed in this study are archived at the Incorporated Research Institutions for Seismology Data Management Center (IRIS DMC) under network codes 2C (*11*) and 1D (*12*).

SUPPLEMENTARY MATERIALS

science.org/doi/10.1126/science.abm3301
Materials and Methods
Figs. S1 to S7
Tables S1 to S3
References (*47–75*)

Submitted 22 September 2021; accepted 2 March 2022
10.1126/science.abm3301

A dynamic saline groundwater system mapped beneath an Antarctic ice stream

Chloe D. GustafsonKerry KeyMatthew R. SiegfriedJ. Paul WinberryHelen A. FrickerRyan A. VenturelliAlexander B. Michaud

Science, 376 (6593), • DOI: 10.1126/science.abm3301

The deeper story

Shallow, dynamic subglacial water systems provide lubrication that facilitates the movement of overlying ice. But are these thin layers the whole story? Gustafson *et al*. show that the subglacial sediments beneath Whillans Ice Stream in West Antarctica are saturated with a mixture of fossil seawater and freshwater from the glacier (see the Perspective by Chu). This groundwater, extending downward for more than a kilometer, contains more than 10 times as much fluid volume as the shallow hydrologic system above and actively exchanges with it. Therefore, it has the potential to modulate ice streaming and subglacial biogeochemical reactions. —HJS

Science (ISSN) is published by the American Association for the Advancement of Science. 1200 New York Avenue NW, Washington, DC 20005. The title *Science* is a registered trademark of AAAS.